Separation Science and Technology
Publication details, including instructions for authors and subscription information:
http://www.informaworld.com/smpp/title~content=t713708471

Particle Deposition in Laminar Crossflow Filtration of Power Law Slurry

Kuo-Jen Hwang[a]; Wei-Ming Lu[b]
[a] DEPARTMENT OF CHEMICAL ENGINEERING, TAMKANG UNIVERSITY TAMSUI, TAIPEI HSIEN, TAIWAN, REPUBLIC OF CHINA [b] DEPARTMENT OF CHEMICAL ENGINEERING, NATIONAL TAIWAN UNIVERSITY, TAIPEI, TAIWAN, REPUBLIC OF CHINA

To cite this Article Hwang, Kuo-Jen and Lu, Wei-Ming(1997) 'Particle Deposition in Laminar Crossflow Filtration of Power Law Slurry', Separation Science and Technology, 32: 8, 1315 — 1334
To link to this Article: DOI: 10.1080/01496399708000963
URL: http://dx.doi.org/10.1080/01496399708000963

SEPARATION SCIENCE AND TECHNOLOGY, 32(8), pp. 1315–1334, 1997

Particle Deposition in Laminar Crossflow Filtration of Power Law Slurry

KUO-JEN HWANG*
DEPARTMENT OF CHEMICAL ENGINEERING
TAMKANG UNIVERSITY
TAMSUI, TAIPEI HSIEN, TAIWAN 25137, REPUBLIC OF CHINA

WEI-MING LU
DEPARTMENT OF CHEMICAL ENGINEERING
NATIONAL TAIWAN UNIVERSITY
TAIPEI, TAIWAN 10617, REPUBLIC OF CHINA

ABSTRACT

A theoretical model for predicting the probability of particle deposition in crossflow filtration of power law slurry is developed. The model is based on the critical angle of friction between depositing particles, which can be estimated by analyzing the forces exerted on the particles. The binding force between the particles due to polymer adsorption plays an important role in the particle deposition. The smaller the flow behavior index of the slurry is, the larger the binding force and the higher the probability of particle deposition will be. The effects of operating conditions such as the crossflow velocity of the slurry and the filtration rate on the probability of particle deposition are also discussed in depth. The calculated values of the probability of particle deposition agree fairly well with the experimental data. A program is designed to simulate the packing structure and the porosity at the cake surface. The porosity increases not only with the increase of the crossflow velocity, but also with the increase of the flow behavior index of the power law slurry.

Key Words. Particle deposition; Crossflow filtration; Power law slurry; Filtration

* To whom correspondence should be addressed.

INTRODUCTION

Crossflow filtration is a highly efficient mode of solid–liquid separation. Since the growth of the filter cake is limited by the high shear stress acting on the surface of the filter septum due to the tangential bulk flow of the slurry, this mode of filtration has many advantages, such as thinner cake thickness, higher filtration rate, longer operation time, etc. It has attracted the attention of both plant engineers and researchers in the field of filtration.

Several kinds of theories for crossflow filtrations have been proposed (1) such as the concentration polarization model (2–4), the particle deposition model (5), and the hydrodynamic model (6–10). However, most researchers limited their focus to Newtonian slurry. The mechanism of the crossflow filtration of power law slurry has not been well studied.

Since many power law fluids are the polymer's aqueous solution, the polymeric molecules may be adsorbed on the particle surfaces during filtration. In the research of Kozicki (11), several phenomena, such as the slipping flow of power law fluid across the particle surfaces, polymer adsorbed on the particle surfaces, and the increase of the flow behavior index of the filtrate, have been observed. Kozicki et al. (12) also found that the adsorption layer of the polymer on the particle surfaces became thicker if the size of the particles or polymeric molecules increased. Recently, by analyzing the forces exerted on the depositing particles, the critical angle of friction between particles in the "dead-end" cake filtration of power law slurry was calculated by Hwang and Lu (13). They also proposed a dynamic method for simulating the packing structure of particles on the cake surface and the variations of local cake properties during the course of filtration.

In crossflow filtration to determine the cake growth rate the size distribution and packing structure of the particles in the filter cake are essential knowledge for grasping the rate of filtration. Lu and Ju (8) proposed a moment balance model for estimating the critical cut-diameter of particles which can deposit stably on the cake surface. Lu and Hwang (10) developed a model based on force balance for calculating the critical angle of friction between depositing particles under various operating conditions. By using this model, the probability of particle deposition and the size distribution of the particles of the cake in a crossflow filtration of Newtonian slurry can be estimated.

In this article the analyses of the author's recent researches (10, 13) are extended to study the probability of particle deposition on the cake surface in the crossflow filtration of power law slurry. A program has also been designed to simulate the packing structure of particles and to estimate the porosity on the cake surface.

THEORY

In this section the forces exerted on particles which stay on the surface of a filter cake are analyzed in order to calculate the value of the critical angle of friction between particles. A theory based on the critical angle of friction is developed to estimate the value of the probability of particle deposition under various conditions. The packing structure and cake porosity can then be simulated.

Critical Angle of Friction between Particles

Figure 1 depicts the deposition of slurry particles onto a cake surface in a two-parallel-plate crossflow filtration system. Particle B in the figure is a particle deposited stably while Particle A is a particle just arriving at the cake surface and touching Particle B. The angle β is known as the "angle of friction." The drags and forces exerted on Particle A caused by fluid flow or other particles of the system can be summarized as: 1) the tangential drag parallel to the filter septum due to slurry flow, F_t; 2) the net drag normal to the filter septum, F_n, which involves the drag due to filtrate flow and the inertial lift force; 3) the net gravity force of the submerged particle, F_g; and 4) the binding force between particles due to the surface adsorption of polymeric molecules, F_i. The force due to Brownian motion of particles is neglected in this study since the diameter of the particles used is larger than 1 μm.

The force balance equation at the critical condition under which Particle A can stick at the position where it touches Particle B is (10)

$$(F_g + F_n) \cos \beta_c + F_t \sin \beta_c = f_c[F_i + (F_g + F_n) \sin \beta_c + F_t \cos \beta_c] \tag{1}$$

where β_c is the critical angle of friction and f_c is the friction coefficient between particles. The left-hand side of Eq. (1) is the net tangential force exerted on Particle A, the direction of which is vertical to the line connecting the two gravity centers of Particles A and B, while the right-hand side is the frictional force between the particles. When $\beta < \beta_c$, the frictional force is larger than the net tangential force; then Particle A will deposit stably at its original position. In contrast, if $\beta > \beta_c$, Particle A will leave the touched location and move until it touches another particle or the

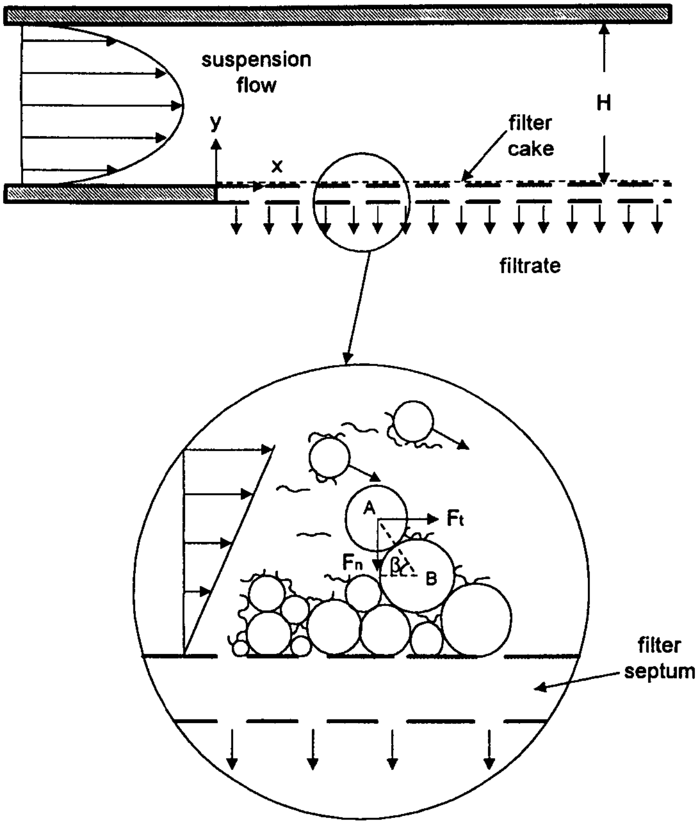

FIG. 1 A two-dimensional crossflow filtration system.

filter septum. Prior to calculating the value of β_c, each term in Eq. (1) should be analyzed.

Tangential Drag Parallel to the Filter Septum

For most crossflow filtrations, the velocity of slurry which flows parallel to the septum is far larger than the permeating velocity of the filtrate. Thus, it can be reasonably assumed that the velocity profile of the tangential fluid flow will not be affected very much by the permeating flow of filtrate and can be expressed as (14)

$$\frac{u}{u_s} = \left(\frac{2n + 1}{n + 1}\right)\left(1 - \left|1 - \frac{2y}{H}\right|^{(n+1)/n}\right) \tag{2}$$

where u_s is the average velocity of the slurry, H is the clearance of the filter channel, and n is the flow behavior index of the power law slurry. At a point very near the filter septum, the velocity profile of the fluid whose direction is parallel to the filter septum may be assumed to be linear; that is, the gradient of velocity and the shear stress acting on the filter septum are

$$\left.\frac{du}{dy}\right|_{y=0} = \frac{u_s}{H}\left(\frac{4n + 2}{n}\right) \tag{3}$$

and

$$\tau_w = -K\left[\frac{u_s}{H}\left(\frac{4n + 2}{n}\right)\right]^n \tag{4}$$

respectively. Compared with the experimental data of Kostic and Hartnett (15), the values of the shear stress acting on the filter septum calculated by Eq. (4) have a deviation of less than 10%. Thus, the apparent viscosity of the power law fluid in the region very near the surface of the filter septum is a constant.

Since the local velocity of the fluid is very low near the filter septum, the tangential drag exerted on Particle A can be evaluated by using the reflection method (16):

$$F_t = 2\pi K a^{2-n}\,[(u_A)^n - (u_{B0A})^n - (u^c_{A0A})^n - (u^c_{B0A})^n] \tag{5}$$

where K is the fluid consistency index, a is the radius of Particle A, u_A is the velocity of Particle A with respect to the fluid flow, u_{B0A} is the reflecting velocity of Particle B on Particle A, and the superscript "c" represents the reflecting velocities owing to the existence of the filter cake. Each reflected velocity is analyzed below.

(1) u_A. According to Eq. (3), the undisturbed velocities at the gravity centers of Particles A and B are

$$u_A = \frac{u_s}{H}\left(\frac{4n + 2}{n}\right)[b + (a + b)\sin\beta] \tag{6}$$

and

$$u_B = \frac{u_s}{H}\left(\frac{4n + 2}{n}\right) b \tag{7}$$

respectively. Thus, the velocity u_A can be obtained from Eq. (6).

(2) u_{BOA}. Extending the analysis of Lu and Hwang (10) for this system, the value of u_{BOA} can be given by

$$u_{BOA}^{n} = u_{B}^{n}\left(\frac{b}{a+b}\right)\left(\frac{3}{2}\cos\beta\,\vec{i} + \frac{3}{4}\sin\beta\,\vec{k}\right) \quad (8)$$

where $\vec{i}$ and $\vec{k}$ are the unit vectors, the directions of which are parallel and vertical to the line connecting with the gravity centers of these two particles, respectively.

(3) u_{AOA}^{c}. From the results of Goldman et al. (17), who calculated the drag exerted on a particle in a couette flow near a plane wall, u_{AOA}^{c} can be given by

$$(u_{AOA}^{c})^{n} = -\frac{9}{16}\left(\frac{a}{b+(a+b)\sin\beta}\right)u_{A}^{n} \quad (9)$$

(4) u_{BOA}^{c}. O'Neill (18) proposed an expression of the tangential drag exerted on a particle which stays on a plane in a simple shear flow:

$$F_{t} = -1.7009[6\pi\eta b u_{B}] \quad (10)$$

where η is the apparent viscosity of the fluid and 1.7009 is the wall correction factor of Stokes' law. Therefore, u_{BOA}^{c} can be given by

$$u_{BOA}^{c} = 1.7009 u_{BOA} \quad (11)$$

Once Eqs. (6), (8), (9), and (11) are substituted into Eq. (5), the tangential drag exerted on Particle A can be estimated.

Net Drag Normal to the Filter Septum

Since the flow rates of the filtrate are very low for most filtrations, the normal drag can also be calculated by using the reflection method, that is,

$$F_{n} = 2\pi K a^{2-n}[(v_{A})^{n} - (v_{BOA})^{n} - (v_{AOA})^{n} - (v_{BOA})^{n}] \quad (12)$$

where v_{A} is the relative velocity between Particle A and the fluid in the direction of filtration and can be calculated by

$$v_{A} = q - v_{l} \quad (13)$$

in which q is the filtration rate and v_{l} is the inertial lift velocity. By solving the Navier–Stokes equations, Vasseur and Cox (19) derived an expression for the lift velocity of a sphere very near a bounded wall in a linear profile of the tangential fluid flow. This can be expressed as

$$v_l = -\frac{61}{576}\left(\frac{\tau_w}{\eta}\right)\left(\frac{d_p}{2}\right)^3 \tag{14}$$

The negative sign on the right-hand side of Eq. (14) is due to the opposite direction of v_l with respect to q.

Each reflecting velocity in Eq. (12) can be calculated by extending the analysis of Hwang and Lu (13) to the "dead-end" cake filtration of power law slurry; therefore, the normal drag exerted on Particle A can be estimated when the rheology of slurry and the operating conditions are given.

Net Gravity of the Submerged Particle

This body force can be simply expressed as

$$F_g = \frac{\pi}{6}(\rho_s - \rho)g d_p^3 \tag{15}$$

where ρ_s and ρ are the densities of the particles and fluid, respectively.

Binding Force between Particles Due to Polymeric Adsorption

The adsorption of polymer molecules on the particle surface due to polymer bridging will result in a binding force between particles (20, 21). This binding force is mainly affected by the dosage of the polymer (21), the configuration of the added polymer (20), and the effective contact area between the polymer and the particles (22). Because this force is often difficult to estimate theoretically, it is measured using various experimental methods. In this study it is assumed for simplicity that this force depends on the concentration of the polymer solute, the shear stress acting on the surface of the filter septum, and the diameter of the particles. Therefore, this force may be expressed as

$$F_i = D(\tau_w, C_s)d_p^m \tag{16}$$

where $D(\tau_w, C_s)$ is a function which depends on the shear stress acting on the surface of the filter septum, τ_w, and the concentration of the polymer solute, C_s. An experimental correlation for Celite 545 particles dispersed in sodium polyacrylate aqueous solution,

$$F_i = 5.45 \times 10^{15}(\tau_w - 2)(C_s - 0.000244)d_p^{3.23} \tag{17}$$

was obtained at 25°C in the range of $C_s < 2000$ ppm and $\tau_w < 6$ N/m^2 in this study.

Once the friction coefficient has been measured by a crossflow filtration system (13, 23), the value of β_c for a given condition can be estimated from Eq. (1).

Probability of Particle Deposition

When a particle is transported and arrives at the cake surface, whether it will deposit or move away is determined by the net force exerted on it. Since the drag exerted on a depositing particle is determined by the point at which it touches the cake surface, there is a probability of deposition for each size of particle under a given operating condition. Once the value of the probability of deposition is known, the size distribution of the deposited particles, which is the main effect on filtration resistance, can be obtained accordingly.

In this study the probability of particle deposition is estimated by using two methods described below.

Calculated from the Value of β_c

The probability of particle deposition can be calculated by the following equation (10):

$$P(d_p) = \frac{\text{the area at which particles can deposit}}{\text{the area to which particles can be transported}} \tag{18}$$

where $P(d_p)$ is the probability function of particle deposition, which is a function of the particle diameter, d_p. Considering particles depositing on a deposited particle such as Particle B shown in Fig. 1, Eq. (18) can be rewritten as

$$P(d_p) = \frac{\beta_c}{\pi/2} \tag{19}$$

for a two-dimensional analysis.

Calculated from Experimental Data

From the results of Shah and Lord (24), one knows that the effect of sedimentation of particles carried by a power law fluid can be neglected in our operating conditions. Thus, it is reasonable to assume that the size distribution of particles which are transported and arrive at the cake surface is the same as that in slurry.

Taking a mass balance for a thin layer located at the surface of a filter cake, one can give (the mass of the particles with a diameter of d_p which are deposited on cake surface in a time period) = (the mass flux of particles arriving at the cake surface in a time period)·(the ratio of particles with a diameter of d_p in the slurry)·(the deposition probability of particles with a diameter of d_p)

or

$$N_w f_c(d_p) d(d_p) = C_0 q f_0(d_p) d(d_p) P(d_p) \tag{20}$$

where N_w is the mass flux of particle deposition, C_0 is the concentration of the slurry, q is the filtration rate, and $f_c(d_p)$ and $f_0(d_p)$ are the frequency functions of the cake and slurry for the particles which have a diameter of d_p, respectively. Equation (20) can be rearranged as

$$P(d_p) = \frac{N_w f_c(d_p)}{C_0 q f_0(d_p)} \tag{21}$$

When the values of N_w, q, $f_c(d_p)$, and $f_0(d_p)$ are measured from experiments, $P(d_p)$ can be obtained by using Eq. (21).

Simulation of Particle Packing on Cake Surface

Based on the calculated value of β_c, the packing structure and porosity at the cake surface can be simulated by a version of the simulation process of Lu and Hwang (10).

EXPERIMENTAL

The crossflow filtrations were carried out by using the two-dimensional crossflow filter shown in Fig. 2. The details of the filter design can be found in the authors' recent paper (9).

Power law fluid was prepared by adding sodium polyacrylate into deionized water. A Celite 545 particulate sample with a mean diameter of 32 μm was gradually dispersed into a sodium polyacrylate aqueous solution using a mechanical stirrer. The filter paper Whatman #2 was used as the filter septum in filtration experiments. A slurry containing 1% Celite by weight was pumped into the filter using a circulation pump, and the concentrated slurry was recycled back into the slurry tank. The clean filtrate received by a receiver was placed on a load cell to determine the amount of filtrate. At the end of each experiment, the flow behavior of the filtrate

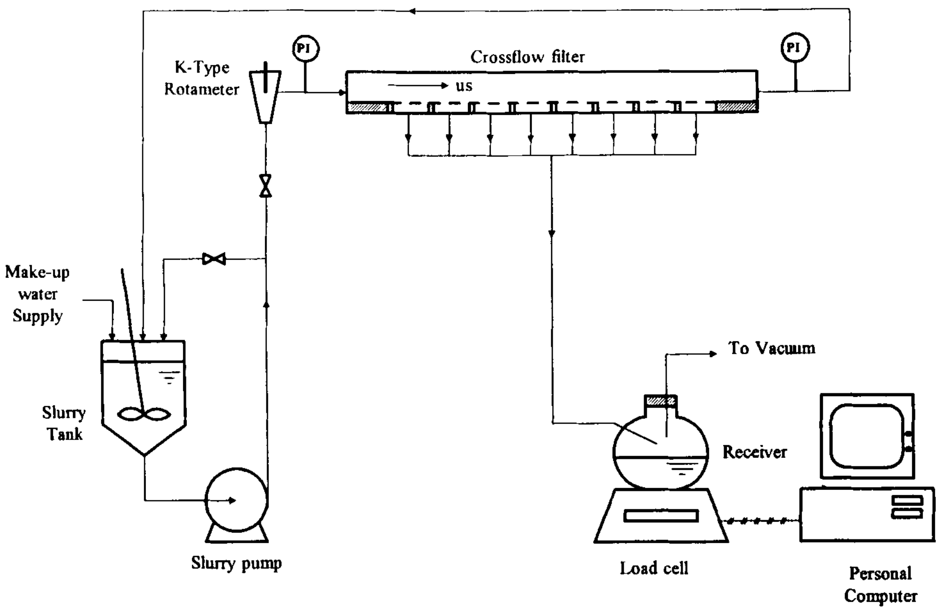

FIG. 2 A schematic diagram of crossflow filtration.

was determined by a Haak viscometer, and the formed cake was carefully scraped and sent to determine its wet and dry mass and to analyze the particle size distribution using a Microtrac optical size analyzer. After several experiments with various terminus times under the same operating condition, the instantaneous mass flux of particle deposition was determined from the slope of the tangent of the curve of the dry cake mass versus time.

RESULTS AND DISCUSSION

Probability of Particle Deposition

The effect of the flow behavior index of the power law slurry on the probability of particle deposition is illustrated in Fig. 3. The values of $P(d_p)$ shown in the figure are calculated using Eq. (19). When the value of n of the slurry decreases, the rate of increase of the tangential drag exerted on the particles at the cake surface is less than that of the net normal drag, and a larger quantity of polymer is dissolved in the slurry, which results in a larger binding force between the particles. Both these

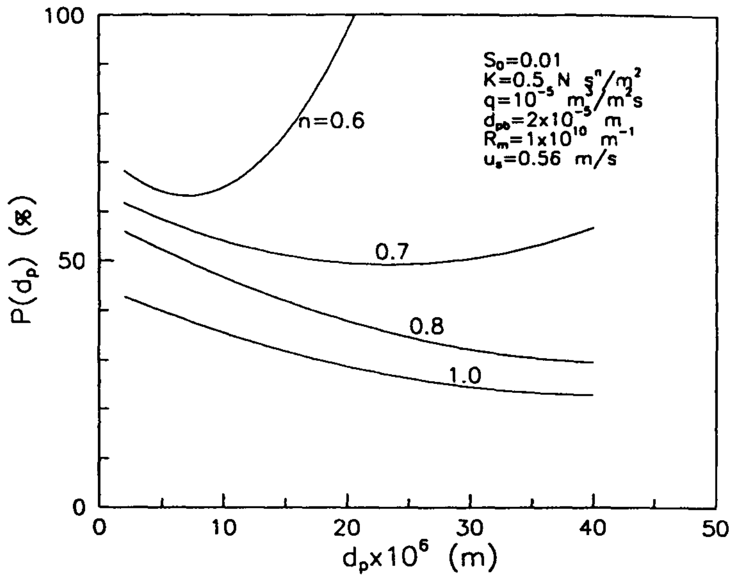

FIG. 3 Effects of flow behavior index and particle size on the probability of particle deposition.

two effects will cause particles to more easily deposit on the cake surface; therefore, the values of $P(d_p)$ increase with the decrease of n for a given operating condition. For the cases of $n = 0.8$ and 1.0, the binding forces are very small compared with the other forces or drags since a small amount of sodium polyacrylate was dissolved in the slurries; thus, the deposition of particles is mainly influenced by the drags exerted on the particles, and the probability will decrease with the increase of the diameter of particles. This tendency is similar to that in the crossflow filtration of Newtonian slurry (10). However, when the value of n decreases, the binding force increases its order of magnitude and plays a more important role in particle deposition. The curve of $n = 0.7$ shows that the value of $P(d_p)$ increases gradually as $d_p > 24$ μm. This is due to the fact that the amount of binding force is proportional to $d_p^{3.23}$ (see Eq. 17). The increase of the binding force causes the particles to more easily deposit when the particle size is greater than 24 μm. For the condition of $n = 0.6$, the influence of the binding force becomes more significant; that is, the value of $P(d_p)$ increases quickly when $d_p > 8$ μm and reaches 100% when $d_p > 22$ μm.

Figure 4 illustrates how the crossflow velocity of slurry affects the value of $P(d_p)$. Just as in Fig. 3, the calculated value of $P(d_p)$ for a given value of u_s will decrease with d_p for small particles and will increase with d_p for large particles. Comparing the curves shown in Fig. 4, it is found that, in the range of $d_p < 30$ μm, the smaller the value of u_s is, the larger the value of $P(d_p)$ will be. This is due to the fact that a smaller u_s will result in a smaller tangential drag and cause a particle to more stably remain at the cake surface. However, in the range of $d_p > 30$ μm, the effect of the binding force is greater than that of the other drags and forces. Since the value of the binding force is proportional to that of the shear stress acting on the cake surface (see Eq. 17), a higher crossflow velocity will result in a larger value of $P(d_p)$ for a given particle size.

Figure 5 shows the calculated values of $P(d_p)$ under various filtration rates. For a given particle diameter, a higher filtration rate will result in a larger normal drag exerted on a particle which stays at the cake surface and will increase the stability of the particle and the value of $P(d_p)$. For a higher filtration rate, e.g., $q = 10^{-4}$ $m^3/m^2{\cdot}s$, the particle deposition is mainly influenced by the frictional drag since $F_d \gg F_i$. Therefore, the tendency of the curve is similar to that of the crossflow filtration of New-

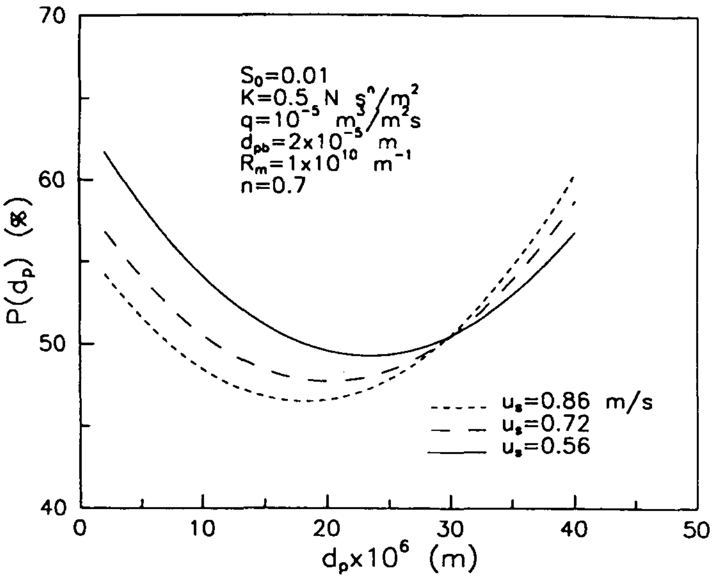

FIG. 4 Effects of crossflow velocity and particle size on the probability of particle deposition.

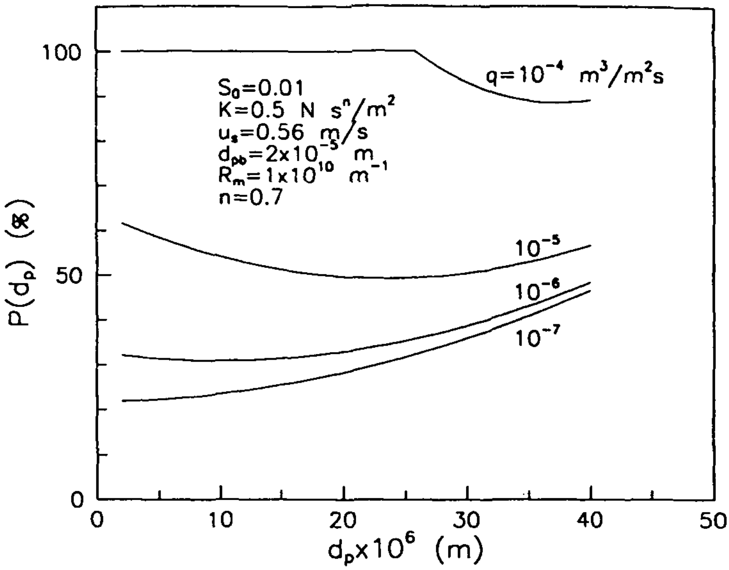

FIG. 5 Effects of filtration rate and particle size on the probability of particle deposition.

tonian slurry (10). A particle with a diameter smaller than the critical value will deposit stably on the cake surface, and the probability of particle deposition will decrease with particle diameter when the particle size exceeds the critical value. However, for a lower filtration rate, the binding force may cause an increase of $P(d_p)$ for a larger particle. For the case of $q = 10^{-7}$ $m^3/m^2 \cdot s$, the value of $P(d_p)$ will increase monotonously with d_p since the binding force will play a dominant role in particle deposition.

The theoretical values and experimental data of $P(d_p)$ are plotted in Fig. 6 to demonstrate the reliability of the proposed theory. The curves shown in the figure are the results calculated by using Eq. (19), while the experimental data were calculated using Eq. (21). Under the operating conditions of this figure, the frictional drag is larger than the binding force; thus, the values of $P(d_p)$ decrease with the increase of d_p. Though the results show good agreement between the calculated and experimental data, there exists a deviation of about 10% for a larger filtration rate. This may be due to a larger number of particles instantaneously arriving at the cake surface for such a case. When a depositing particle is obstructed by other particles during deposition, it has more opportunity to stay on the cake surface. Therefore, the predicted values of $P(d_p)$ may be underestimated for larger filtration rates.

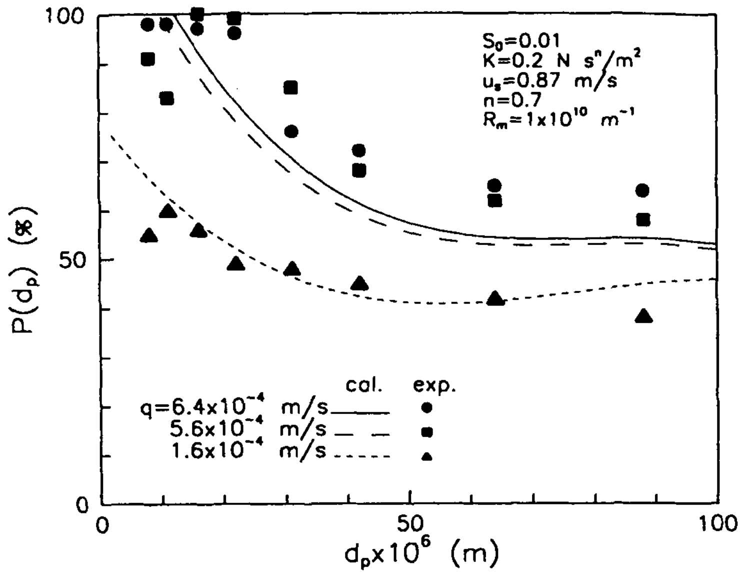

FIG. 6 Comparison of probability of particle deposition between the experimental data and calculated results.

Packing Structure of Particles and Porosity at the Cake Surface

The version of the simulation process of Lu and Hwang (10) was carried out to simulate the packing structures of particles at the initial stage of crossflow filtration. Figures 7(a)–(c) show the simulated packing structures of spherical particles whose size distribution is the same as that of Celite 545 used in experiments under the same conditions as those in Fig. 3 for three different values of n. It can be found from the figures that the particles are packed at an angle with respect to the direction of filtration, which is similar to those in crossflow filtration of Newtonian slurry (10). Furthermore, since the probability of particle deposition increases with the decrease of flow behavior index (from Fig. 3), a larger quantity of particles will deposit to form a more compact cake under a smaller value of flow behavior index.

Figure 8 shows the simulated porosity at the initial stage of deposition of spherical particles under various n. The regressing curve shown in the figure illustrates that ϵ_i increases almost linearly with the increase of n. This tendency is similar to that of cake filtration of power law slurry (13).

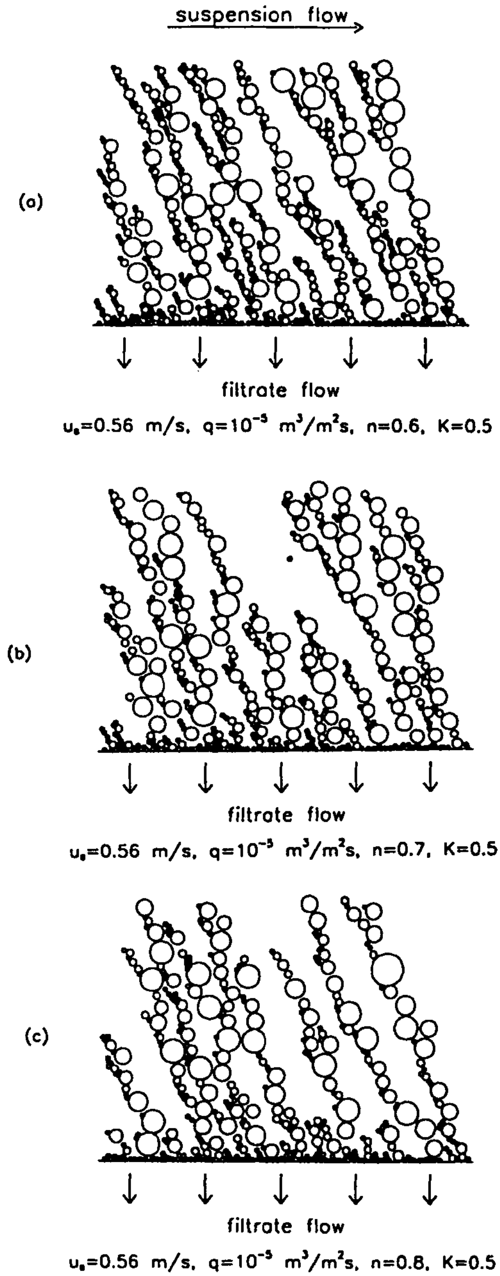

FIG. 7 Simulated packing structures of particles on the cake surface under various flow behavior indexes.

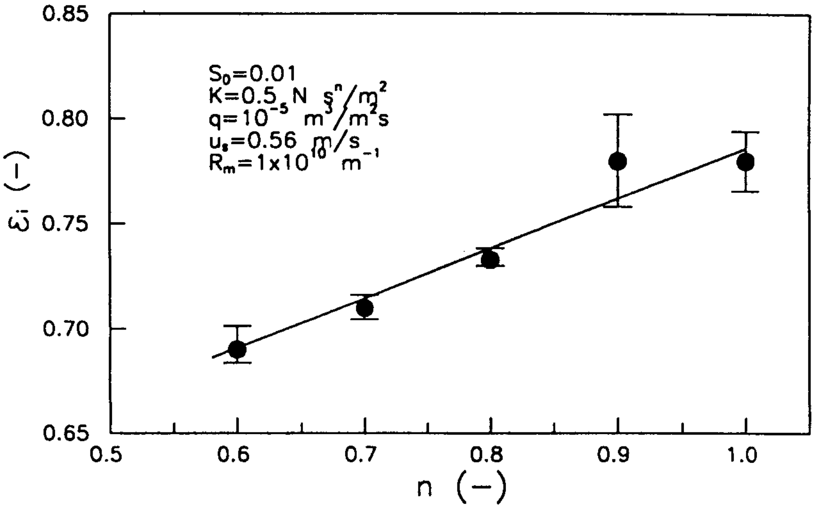

FIG. 8 Effects of flow behavior index on the packing porosity of spherical particles.

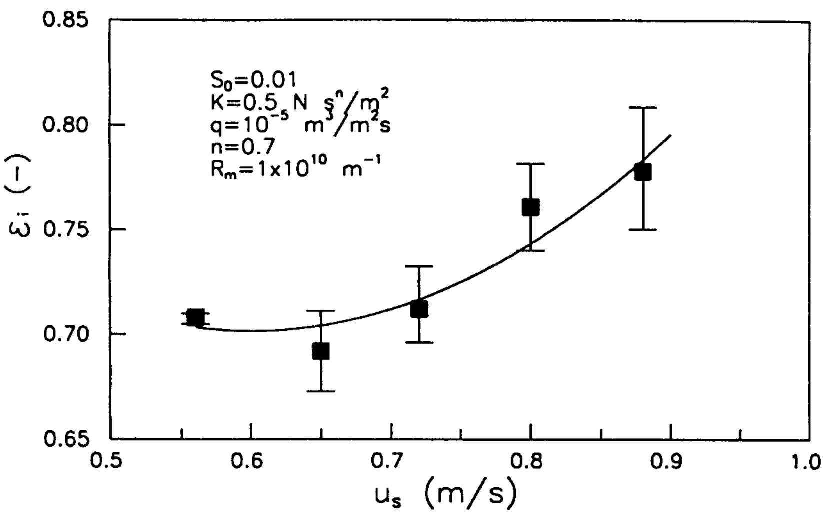

FIG. 9 Effects of crossflow velocity on the packing porosity of spherical particles.

Figure 9 illustrates how the crossflow velocity affects the packing porosity of particles at the cake surface. Since the increase of u_s will decrease the value of $P(d_p)$ and the size distribution of particles in the cake, these effects will increase the porosity of particles packed at the cake surface (10). Therefore, the regressing curve shows that the higher the crossflow velocity is, the larger the cake porosity will be. However, for a low value of u_s such as $u_s < 0.7$ m/s, the effect of the binding force on the particle deposition becomes more important and results in larger values of $P(d_p)$, the size distribution of particles in the cake, and porosity for a smaller u_s. As a result, the smallest value of cake porosity exists at $u_s = 0.65$ m/s.

In general, the value of specific filtration resistance of a cake will be determined by the size and the physical properties of particles and the porosity of the filter cake. When the cake porosity and the size distribution of particles have been known by using the method proposed by this study, the filtration resistance and the steady flux can then be estimated.

CONCLUSION

By analyzing the forces and drags exerted on depositing particles, the values of the critical angle of friction between particles under various conditions have been determined. The calculated value of the critical angle of friction has been used to estimate the probability of particle deposition and has been used to simulate the packing structure on the cake surface. Filtration of a slurry with a smaller flow behavior index will result in a larger probability of particle deposition for a given particle size and in a larger value of packing porosity on the cake surface. The binding force between the particles due to polymer adsorption plays an important role in particle deposition when its order of magnitude is the same as that of the frictional drag exerted on the particles. A larger binding force will cause the particles to deposit more stably on the cake surface and to pack into a more compact cake. The binding force may also cause a large particle to have a larger value for the probability of particle deposition compared to that of a small particle. This phenomenon is very different from that in the crossflow filtration of Newtonian slurry, in which the probability of particle deposition decreases monotonously with the increase of particle size. The effects of operating conditions such as the crossflow velocity and filtration rate on the probability of particle deposition and on the packing porosity at the cake surface have also been discussed in depth. The porosity at the cake surface increases not only with the increase of the crossflow velocity, but also with the increase of the flow behavior index of the power law slurry. The calculated values of the probability of particle deposition agree fairly well with the experimental data.

ACKNOWLEDGMENT

The authors express their sincere gratitude to the National Science Council of the Republic of China for its financial support.

NOMENCLATURE

a	radius of Particle A (m)
b	radius of Particle B (m)
C_0	concentration of slurry (kg/m^3)
C_s	concentration of polymer (ppm)
d_p	diameter of particles (m)
f_c	frictional coefficient (—)
$f_c(d_p)$, $f_0(d_p)$	frequency functions of cake and slurry for the diameter d_p, respectively (—)
F_g	gravity force (N)
F_i	binding force between particles (N)
F_n	normal drag exerted on particles (N)
F_t	tangential drag exerted on particles (N)
g	acceleration of gravity (m/s^2)
H	clearance of the filter (m)
$\vec{i}$, $\vec{k}$	the unit vectors, the directions of which are parallel and vertical to the line connecting the gravity centers of two specified particles
K	fluid consistency index (N·s^n/m^2)
n	flow behavior index (—)
N_w	mass flux of particle deposition (kg/m^2·s)
$P(d_p)$	probability of particle deposition (%)
q	filtration rate (m^3/m^2·s)
R_m	filtration resistance of the filter septum (1/m)
s	mass fraction of solid in slurry (—)
t	filtration time (s)
u	tangential velocity of slurry (m/s)
u_s	average crossflow velocity of slurry (m/s)
v	permeating velocity of filtrate (m/s)
v_l	inertial lift velocity (m/s)
y	distance from the surface of filter septum (m)

Greek Letters

β	friction angle between particles (rad)
ϵ_i	porosity at cake surface (—)

η apparent viscosity of power law fluid ($N \cdot s/m^2$)
ρ_s density of particles (kg/m^3)
ρ density of fluid (kg/m^3)
τ_w shear stress on the filter septum (N/m^2)

Subscripts

a Particle A
b Particle B
c critical condition
s slurry

REFERENCES

1. V. Gekas and B. Hallstrom, "Microfiltration Membranes, Cross-Flow Transport Mechanisms and Fouling Studies," *Desalination*, *77*, 195–218 (1990).
2. M. C. Porter, "Ultrafiltration of Colloidal Suspensions," *AIChE Symp. Ser.*, *68*(120), 21 (1972).
3. C. A. Romero and R. H. Davis, "Global Model of Crossflow Microfiltration Based on Hydrodynamic Particle Diffusion," *J. Memb. Sci.*, *39*, 157 (1988).
4. C. A. Romero and R. H. Davis, "Transient Model of Crossflow Microfiltration," *Chem. Eng. Sci.*, *45*, 13 (1990).
5. R. D. Cohen and R. F. Probstein, "Colloidal Fouling of Reverse Osmosis Membranes," *J. Colloid Interface Sci.*, *114*, 194–207 (1984).
6. G. Belfort, "Fluid Mechanics in Membrane Filtration: Recent Developments," *J. Membr. Sci.*, *40*, 123 (1989).
7. C. Kleinstreuer and M. S. Paller, "Laminar Dilute Suspension Flow in Plate-and-Frame Ultrafiltration Units," *AIChE J.*, *29*(4), 529 (1983).
8. W. M. Lu and S. C. Ju, "Selective Particle Deposition in Cross-Flow Filtration," *Sep. Sci. Technol.*, *24*, 517–540 (1989).
9. W. M. Lu, K. J. Hwang, and S. C. Ju, "Studies on the Mechanism of Cross-Flow Filtration," *Chem. Eng. Sci.*, *48*(5), 863–872 (1993).
10. W. M. Lu and K. J. Hwang, "Cake Formation in 2-D Cross-Flow Filtration," *AIChE J.*, *41*(6), 1443–1455 (1995).
11. W. Kozicki, "Recent Developments in Filtration of Non-Newtonian Fluids," *Proc. Filtr. Symp. Nagoya '86*, 121–130 (1986).
12. W. Kozicki, M. R. Hanna, and C. Tiu, "Polymer Adsorption in Packed Bed Flow," *J. Rheol.*, *32*(6), 593–619 (1988).
13. K. J. Hwang and W. M. Lu, "Dynamic Analysis on Constant Pressure Filtration of Power Law Slurry," *J. Chem. Eng. Jpn.*, *29*(1), 65–74 (1996).
14. S. C. Ju, "A Study on the Mechanism of Cross-Flow Filtration," Ph.D. Dissertation, Department of Chemical Engineering, National Taiwan University, Republic of China, 1989.
15. M. Kostic and J. P. Hartnett, "Predicting Turbulent Friction Factors of Non-Newtonian Fluid in Noncircular Ducts," *Int. Comm. Heat Mass Transfer*, *11*, 345 (1984).
16. J. Happel and H. Brenner, *Low Reynolds Number Hydrodynamics*, Prentice-Hall, Englewood Cliffs, NJ, 1965, Chap. 6–8.

17. A. J. Goldman, R. G. Cox, and H. Brenner, "Slow Viscous Motion of a Sphere Parallel to a Plane Wall—II. Couette Flow," *Chem. Eng. Sci.*, *22*, 653–660 (1967).
18. M. E. O'Neill, "A Sphere in Contact with a Plane Wall in a Slow Linear Shear Flow," *Ibid.*, *23*, 1293 (1968).
19. P. Vasseur and R. G. Cox, "The Lateral Migration of Spherical Particle in Two Dimensional Shear Flow," *J. Fluid Mech.*, *78*, 385 (1976).
20. J. Gregory, "Kinetic Aspects of Polymer Adsorption and Flocculation," in *Flocculation in Biotechnology and Separation Systems* (Y. A. Attia, Ed.), Elsevier Science, Amsterdam, 1987.
21. S. Levine and W. I. Friesen, "Flocculation of Colloid Particles by Water-Soluble Polymers," in *Flocculation in Biotechnology and Separation Systems* (Y. A. Attia, Ed.), Elsevier Science, Amsterdam, 1987.
22. J. Eisenlauer and D. Horn, "Influence of Shear and Salt on Flocculation in Laminar Tube Flow," in *Solid-Liquid Separation* (J. Gregory, Ed.), Ellis Horwood, England, 1984, Chap. 14.
23. W. M. Lu and K. J. Hwang, "Mechanism of Cake Formation in Constant Pressure Filtration," *Sep. Technol.*, *3*, 122–132 (1993).
24. S. N. Shah and D. L. Lord, *Slurry Transport in Horizontal Pipes with Non-Newtonian Carrier Fluids*, Paper No. 1003ck, AIChE Annual Meeting, November 5–10, 1989, San Francisco, CA, USA.

Received by editor June 5, 1996
Revision received October 17, 1996